Reac Kinet Mech Cat (2017) 120:295–305
DOI 10.1007/s11144-016-1094-6

Ordered mesoporous Sn–TiO_2 catalysts via an evaporation induced self-assembly method for the Baeyer–Villiger oxidation of cyclohexanone by molecular oxygen

Zhiwei Zhou[1] · Yang Yu[1] · Pengcheng Yu[1] · Juan Qin[2] · Songshan Dai[1] · Wenliang Wu[1]

Received: 11 August 2016 / Accepted: 11 October 2016 / Published online: 25 October 2016

Abstract In order to improve the catalytic performance in the Baeyer–Villiger oxidation of cyclohexanone by molecular oxygen, ordered mesoporous Sn–TiO_2 catalysts with high Lewis acidity were successfully designed and synthesized via a facile one-pot evaporation induced self-assembly method. Their physical and chemical properties were characterized by different techniques including XRD, N_2 adsorption–desorption, UV–Vis spectra, ICP, Py-IR, SEM and TEM. The XRD, TEM and N_2 adsorption–desorption results showed that the ordered mesoporous structure can be preserved after tin incorporation. The UV–Vis, SEM and Py-IR results indicated that tin species can be homogeneously tetrahedrally incorporated in the crystalline framework of mesoporous anatase TiO_2 and create the Lewis acidity. The ordered mesoporous 15Sn–TiO_2 catalyst showed highest catalytic performance where cyclohexanone conversion of 91.4 % and ε-caprolactone selectivity of 93.2 %. Moreover, catalytic recycling tests demonstrated that the Sn–TiO_2 catalysts exhibited high potential reusability.

Keywords Ordered mesoporous Sn–TiO_2 · Cyclohexanone · Baeyer–Villiger oxidation · Molecular oxygen

Introduction

The Baeyer–Villiger (B–V) oxidation reaction provides a method for converting ketones to their corresponding lactones or esters, which inspired great interests due to their extensive potential applications for fine chemicals, pharmaceuticals and

✉ Wenliang Wu
wwl@njtech.edu.cn

[1] College of Chemical Engineering, Nanjing Tech University, Nanjing 210009, China

[2] Technology and Finance Service Center of Jiangsu Province, Productivity Center of Jiangsu Province, Nanjing 210042, China

polyesters etc. [1–4]. In the traditional industrial process, different types of explosive and corrosive peroxyacids are usually applied, which would cause a huge amount of toxic by-products resulting in the difficult separation and environmental pollution [5–7]. To meet green chemistry requirements, many efforts have been made to synthesize ε-caprolactone by B–V oxidation of cyclohexanone with hydrogen peroxide and molecular oxygen. However, molecular oxygen can act as a more suitable oxidant because it was safe and cheap as well as less corrosion to equipment [8–10].

Mesoporous materials with regular mesopores have been regarded as promising supports or catalysts because of their high surface areas and large pore volumes [11–13], and the catalytic performance in many catalytic processes, including oxidation, alkylation and esterification etc., can be promoted by the incorporation of different heteroatoms into the framework of the mesoporous materials [14]. Sn-doped microporous and mesoporous materials, such as Sn-β and Mg/Al/Sn hydrotalcite-like oxides etc. [15, 16], can create the Lewis sites, which can activate the carbonyl group of cyclohexanone [17, 18] and would act as efficient and stable heterogeneous catalyst for the Baeyer–Villiger oxidation. However, the catalytic performance would be dropped because the mesoporous framework with higher loading of tin species would be partially collapsed [19]. Therefore, it is essential to seek a suitable mesoporous material for higher incorporation of tin species, which can act as a promising catalyst in the B–V oxidation of cyclohexanone by molecular oxygen.

Mesoporous TiO_2, as a typical mesoporous material, has been widely used in various catalytic reactions owing to its excellent chemical and thermal stability [20–22], and many transition metal species (Cu, Fe, Cr, etc.) can be easily and successfully incorporated because of its mesoporous framework with reducible active oxygen species [20, 23–25]. At the same time, the small influence by incorporation of tetravalent tin (Sn^{4+}) on the mesoporous framework of TiO_2 would be probably formed owing to the similar ionic radius of Sn^{4+} (0.069 nm) and Ti^{4+} (0.061 nm) as well as their equal charges. In addition, the mesoporous TiO_2 can accept the lone-pair electron by its *3d* empty orbitals, which can also activate the carbonyl group with nucleophilic attack [26]. Based on the above-mentioned opinions, the multicomponent mesoporous Sn–TiO_2 materials via the evaporation induced self-assembly (EISA) method raised by Grosso, which has been acknowledged as the most simple and facile method for the preparation of ordered mesoporous metal oxides [27, 28], would be hopefully as a promising catalyst with higher catalytic performance in the B–V oxidation of cyclohexanone by their synergistic effect. To the best of our knowledge, this is the first report for such a one-pot synthesis of ordered mesoporous Sn–TiO_2 catalyst with amount of Lewis acidity for the B–V oxidation of cyclohexanone by molecular oxygen.

Herein, a series of ordered mesoporous Sn–TiO_2 catalysts are prepared by a facile one-pot EISA strategy, and the physical and chemical properties are characterized by XRD, N_2 adsorption–desorption, ICP, Py-IR, UV–Vis spectra, SEM and TEM techniques. In addition, these synthesized catalysts are employed in the B–V oxidation of cyclohexanone by molecular oxygen, and the catalytic reusability is also investigated.

Experimental

Catalysts preparation

Mesoporous Sn–TiO_2 catalysts are synthesized according to the literature [29]. In a typical synthesis process, 1.6 g of F127, 0.6 g of citric acid and 1.4 g of hydrochloric acid were dissolved into 30 g anhydrous ethanol. After that, 3 g of titanium isopropoxide and a demanded amount of tin tetrachloride (0, 0.18, 0.23, 0.29 and 0.35 g) were simultaneously added into the above solution and vigorously stirred at 303 K for 24 h. The solution was transferred to a Petri dish to evaporate at 318 K for 48 h and then thermally treated at 373 K for another 24 h. The catalysts was collected by calcination in air at 623 K for 5 h to remove the organic template and defined as xSn–TiO_2, where x stands for the weight percent of tin species in the catalysts.

Catalysts characterization

The low-angle and wide-angle XRD patterns of the catalysts in the 2θ range from 0.75° to 5° and from 10° to 80° were obtained on a Bruker D8 instrument with Ni-filtered Cu K_α radiation ($\lambda = 0.154$ nm) and operated at 40 kV, 40 mA when the scanning rate was 0.05°/s. Nitrogen adsorption–desorption isotherms were obtained using Bel Japan Inc.. The surface area was calculated by the BET method and the mesoporous size distribution was obtained by the BJH adsorption model. The weight percent of tin species was analyzed by ICP (Optima 2100 DV, PerkinElmer, USA) after the catalysts had been dissolved in HF solution. UV–Vis DRS for the catalysts were measured on Lambda 950 spectrophotometer. The wavelength range was from 200 to 800 nm and the $BaSO_4$ was as a reference compound. FT-IR spectra of pyridine (Py-IR) were obtained on the Thermo Nicolet Nexus spectrometer in KBr pellets. The catalysts was pretreated in 10^{-2} Pa at 573 K for 3 h and then cooled down to room temperature. After that, pyridine was adsorbed for 2 h and the temperature was raise to 473 K for 1 h to remove the physisorbed pyridine. IR spectra were measured when the temperature of the catalyst was room temperature. The morphology of the catalysts was visualized using a JEOL JEM 2100 TEM operated at 120 kV. The catalysts were dispersed in ethanol assisted by an ultrasonic technique. The dispersion of the semi-quantitative elemental composition (Sn, Ti) was verified by energy dispersive X-ray (EDX) spectrometer in the Oxford INCA EDAX Detecting Unit.

Catalytic activity test

The catalytic performance of the synthesized catalysts were investigated in the B–V oxidation of cyclohexanone by molecular oxygen, which was carried out in a three-neck flat bottom flask equipped with a reflux condenser at atmospheric pressure. In a typical process, 0.12 g catalyst and 1.2 g benzaldehyde as pro-oxygenic agent were simultaneously added into the solution containing of 0.5 g cyclohexanone and 15 g

acetonitrile as solvent. Subsequently, molecular oxygen was introduced to the reaction system at a rate of 10 mL/min. The solution was raised up to 343 K and kept for 5 h with continuous stirring. After that, the flask was cooled down to room temperature and the reaction mixture was analyzed on a SP-6890 gas chromatograph equipped with a SE-30 column (0.25 μm × 50 m) and a flame ionization detector (FID). The cyclohexanone conversion and ε-caprolactone selectivity were calculated when dodecane was the internal standard. The reuse ability of the catalyst was investigated by filtration without any treatment in the recycling tests.

Results and discussion

Catalysts characterization

The XRD patterns for different *x*Sn–TiO_2 catalysts are shown in Fig. 1. It can be seen from Fig. 1a that compared to pure mesoporous TiO_2 catalyst, one obvious diffraction peak centered at around 1.2 ° can be obviously observed for mesoporous *x*Sn–TiO_2 catalysts, suggesting their short-range ordered mesoporous characters [30]. In addition, the peak intensity for *x*Sn–TiO_2 catalysts decreased slightly with the weight percent of tin species increasing from 9 to 15 and the peak was shifted to lower angles indicating that the mesoporous structure can be kept well and the interplanar spacing increased on the basis of the Bragg equation [31]. However, the peak intensity for 18Sn–TiO_2 catalyst severely decreased because of the partial destruction of ordered mesoporous structure by excess tin species probably. As can be seen from Fig. 1b, the pure crystalline anatase TiO_2 was observed and the intensities of these diffraction peaks decreased by the introduction of tin species [32]. It is interesting to note that no significant characteristic peak corresponding to tin-containing compounds such as SnO_2 or Sn_xTiO_y can be found, which may be owing to the highly dispersion of tin species or their homogeneous incorporation into the framework of mesoporous anatase TiO_2 [33].

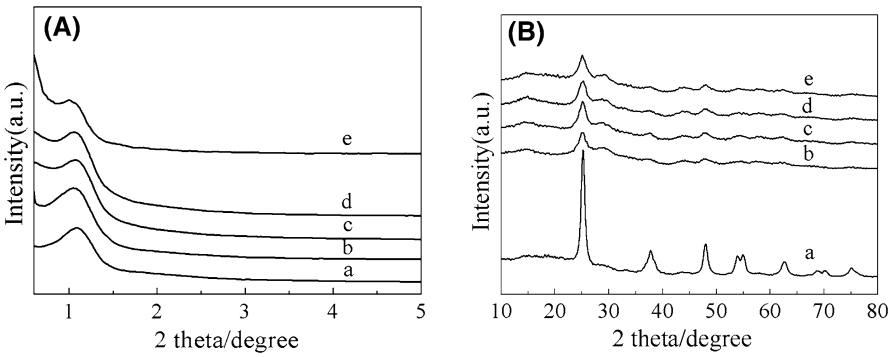

Fig. 1 Small-angle (**a**) and wide-angle (**b**) XRD patterns for (*a*) TiO_2, (*b*) 9Sn–TiO_2, (*c*) 12Sn–TiO_2, (*d*) 15Sn–TiO_2 and (*e*) 18Sn–TiO_2 catalysts

The physical properties for the synthesized xSn–TiO_2 catalysts were characterized by N_2 adsorption–desorption. Fig. 2 shows the N_2 adsorption–desorption isotherms and pore size distribution. It can be clearly seen from Fig. 2 that a typical IV-type isotherms with well-defined H_2 hysteresis loops and sharp capillary condensation steps at a relative pressure ranging from 0.40 to 0.70 for all the catalysts, which indicated that they have a uniform mesoporous system [34], whose pore sizes were narrowly around at 4–5 nm. Some physical data are listed in Table 1. The surface area, pore size and pore volume increased with the weight percent of tin species increasing from 0 to 15 because of its larger interplanar spacing proposed by the small angle XRD patterns. The drop of specific surface area for 18Sn–TiO_2 catalyst may be owing to the partial destruction of the structure, which is coincident with the results of XRD patterns. In addition, the actual loading of tin species was found to be almost agreed with the targeted values based on the ICP results.

Fig. 3 is the TEM images for 15Sn–TiO_2 catalyst. As can be seen from Fig. 3a, the typical regular mesoporous system was obviously observed, which was in good agreement with the small-angle XRD patterns. The mesoporous framework of anatase TiO_2 is crystallized with lattices in the d-spacing of 0.346 nm from the HR-TEM image shown in Fig. 3b, which is well-matched to the 101 reflection [20]. Meanwhile, the lattice fringes 0.211 nm assigned to the Sn species can be observed [35], which can be concluded that tin species can be homogeneously incorporated into the framework of mesoporous anatase TiO_2 based on the results of wide-angle XRD patterns.

In order to clarify the type or coordination state of tin species in the xSn–TiO_2 catalysts, the typical UV–Vis DRS technique was employed and the results are shown in Fig. 4. It can be seen that two obvious absorption bands centered at around 220 and 310 nm for TiO_2 catalyst can be observed [36]. Compared to TiO_2, a red shift of absorption bands for xSn–TiO_2 catalysts can be observed, which is probably owing to the reduced crystallinity by XRD analysis [37]. A new band centered at around 210 nm and no obvious absorption band centered at 400 nm corresponding to bulk SnO_2 particles can be observed, suggesting that tin species would be

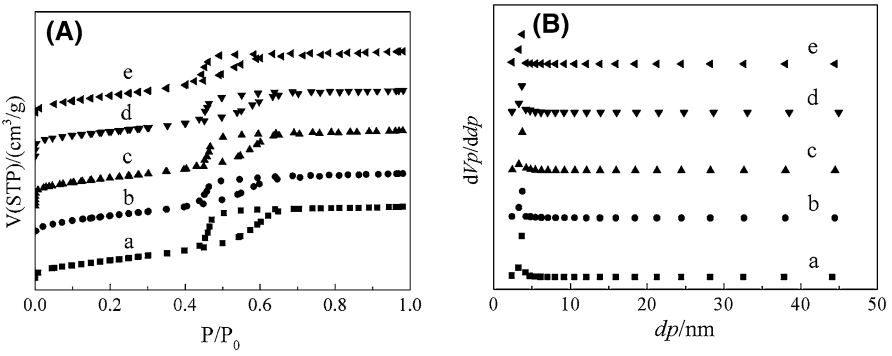

Fig. 2 N_2 adsorption–desorption isotherms (**a**) and pore size distribution (**b**) for (*a*) TiO_2, (*b*) 9Sn–TiO_2, (*c*) 12Sn–TiO_2, (*d*) 15Sn–TiO_2 and (*e*) 18Sn–TiO_2 catalysts

Table 1 Physical properties for different xSn–TiO_2 catalysts

Catalysts	Pore size (nm)[a]	S_{BET} (m^2/g)[b]	Pore volume (cm^3/g)[c]	Sn loading (wt%)[d]
TiO_2	4.0	108.5	0.15	0.0
9Sn–TiO_2	4.5	129.3	0.16	8.93
12Sn–TiO_2	4.6	139.5	0.18	12.01
15Sn–TiO_2	4.8	141.4	0.19	14.98
18Sn–TiO_2	5.5	117.7	0.22	17.97

[a] BJH method

[b] BET specific areas

[c] $P/P_0 = 0.99$

[d] ICP-OES

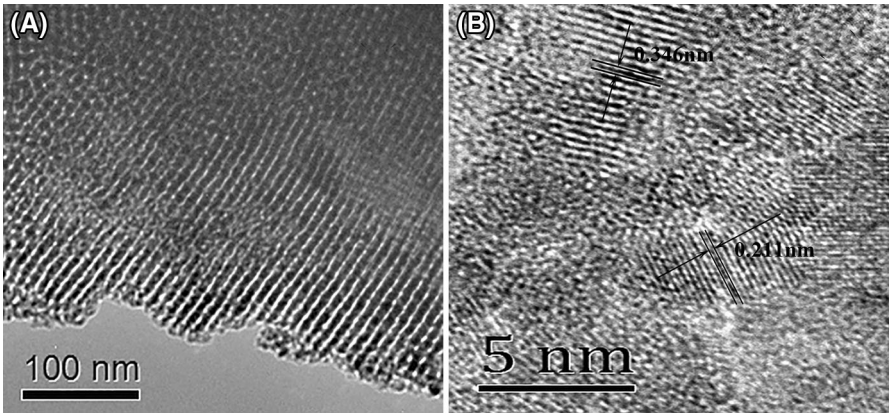

Fig. 3 TEM images for 15Sn–TiO_2 catalyst

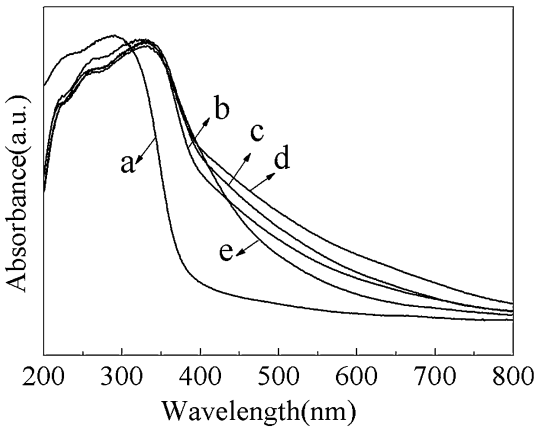

Fig. 4 UV–Vis spectra for (*a*) TiO_2, (*b*) 9Sn–TiO_2, (*c*) 12Sn–TiO_2, (*d*) 15Sn–TiO_2 and (*e*) 18Sn–TiO_2 catalysts

homogeneously tetrahedral incorporated into the framework of mesoporous anatase TiO_2 supports [38].

Fig. 5 is the SEM photo and election mapping of particles for 15Sn–TiO_2 catalyst. It can be seen that a conchoidal morphology was obtained. The element mapping of the 15Sn–TiO_2 catalyst confirmed that Sn species are homogeneously dispersed on the catalyst surface, which agreed to the XRD analysis and UV–Vis DRS spectra.

Py-IR spectra for different xSn–TiO_2 catalysts are shown in Fig. 6. The bands at 1455 and 1545 cm^{-1} could be assigned to the effects between pyridine and Lewis and Brønsted acid sites, respectively [39]. It can be seen that all the xSn–TiO_2 catalysts mainly have Lewis acid sites and it would be promoted by the tetrahedrally incorporated tin species based on the UV–Vis spectra. At the same time, the Lewis acidity increases with the weight percent of tin species increasing, which would be beneficial to their catalytic performances in the oxidation of cyclohexanone by molecular oxygen.

Catalyst performance

Table 2 shows the summary of catalytic performances of different xSn–TiO_2 catalysts in the B–V oxidation of cyclohexanone by molecular oxygen. It can be seen that the ε-caprolactone cannot be found when the reaction was conducted in the absence of benzaldehyde, suggesting its extremely low oxidation capacity of molecular oxygen [40]. However, a cyclohexanone conversion of 36.2 % and ε-caprolactone selectivity of 81.9 % can be obtained when the benzaldehyde was added into the reaction system even though it was carried out without catalyst, which indicates that the benzaldehyde is essential for the B–V oxidation of cyclohexanone by molecular oxygen [41]. Further, cyclohexanone conversion of 78.3 % and ε-caprolactone selectivity of 84.2 % can be obtained for pure mesoporous TiO_2 catalyst, owing to its *3d* empty orbital, which can activate the carbonyl group with nucleophilic attack [26]. Both cyclohexanone conversion and ε-caprolactone selectivity would be promoted after the incorporation of tin species, which attributes to increased Lewis acid between the tin species and the TiO_2 supports probably. And cyclohexanone conversion can reach maximum 91.4 %, which is higher than that of carbon materials [40], mesoporous Mg–Al mixed oxides [10], when the 15Sn–TiO_2 sample was catalyst, owing to its appropriate BET surface area, pore volume and Lewis acidity probably. With the weight percent of tin species further increasing to 18 %, cyclohexanone conversion

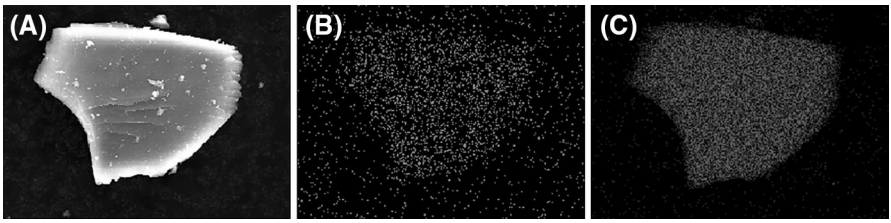

Fig. 5 SEM image of the 15Sn–TiO_2 catalyst (**a**), elemental mapping images of Sn (**b**), and Ti (**c**)

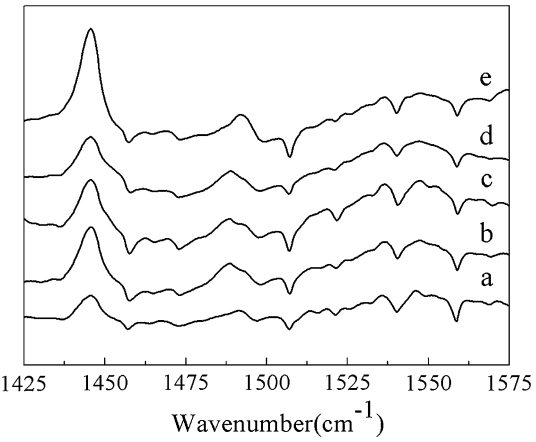

Fig. 6 Py-IR spectra for (*a*) TiO_2, (*b*) 9Sn–TiO_2, (*c*) 12Sn–TiO_2, (*d*) 15Sn–TiO_2 and (*e*) 18Sn–TiO_2 catalysts

Table 2 Catalytic performances of different *x*Sn–TiO_2 catalysts in the B–V oxidation of cylcohexanone by molecular oxygen

Entry	Catalysts	Cyclohexanone conversion (%)	ε-caprolactone selectivity (%)
1[a]	15Sn–TiO_2	–	–
2	None	36.2	81.9
3	TiO_2	78.3	84.2
4	9Sn–TiO	85.4	86.6
5	12Sn–TiO_2	88.3	90.7
6	15Sn–TiO_2	91.4	93.2
7	18Sn–TiO_2	89.6	91.8

Reaction conditions: w(catalyst)/w(cyclohexanone) = 0.24; w(acetonitrile)/w(cyclohexanone) = 30; w(benzaldehyde)/w(cyclohexanone) = 2.4; reaction time: 5 h; O_2: 10 mL/min; reaction temperature: 343 K

[a] Conducted in the absence of benzaldehyde

and ε-caprolactone selectivity decreased because of its loss of surface area probably even though it has excess Lewis acid amount.

Table 3 is the reusable ability for 15Sn–TiO_2 catalyst in the B–V oxidation of cyclohexanone by molecular oxygen. As seen from Table 3, the conversion of cyclohexanone and selectivity of ε-caprolactone declines slightly with the reaction number increasing. Conversion of cyclohexanone 88.7 % and selectivity of ε-caprolactone 90.8 % can be obtained after repeated reaction for 5 times, indicating that the 15Sn–TiO_2 catalyst has good reusable ability because it was only collected by filtration without any treatment in the next reaction number.

The possible reaction mechanism

Reaction mechanism for B–V oxidation of cyclohexanone by molecular oxygen has been widely studied and a two-step mechanism was proposed in the previous

Table 3 The reusable ability for 15Sn–TiO_2 sample in the B–V oxidation of cyclohexanone by molecular oxygen

Reaction number	Cyclohexanone conversion (%)	ε-caprolactone selectivity (%)
1	91.4	93.2
2	90.8	92.6
3	89.9	91.8
4	89.1	91.1
5	88.7	90.8

Reaction conditions: w (15Sn–TiO_2)/w (cyclohexanone) = 0.24; w (acetonitrile)/w (cyclohexanone) = 30; w (benzaldehyde)/w (cyclohexanone) = 2.4; reaction time: 5 h; O_2: 10 mL/min; reaction temperature: 343 K

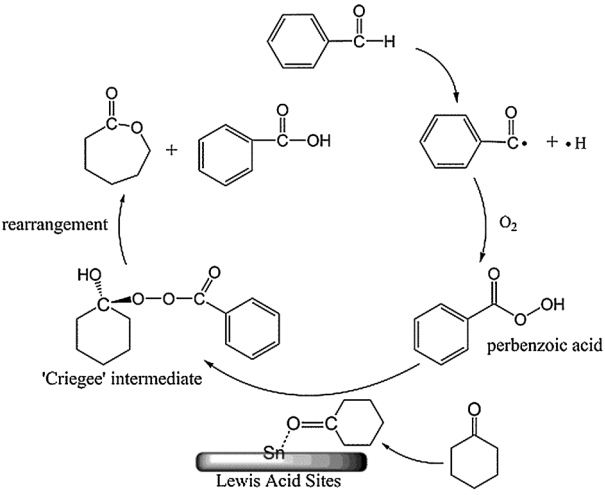

Scheme 1 Possible reaction mechanism for the Baeyer–Villiger oxidation of cyclohexanone by molecular oxygen

literatures [41–44]. In order to clarify the effect of benzaldehyde in the reaction system, its oxidation by molecular oxygen was carried out. The yield of benzoic acid was almost the same regardless of Sn–TiO_2 catalyst (not shown here), suggesting that the negligible effect on the oxidation of benzaldehyde over Sn–TiO_2 catalyst can be obtained. Therefore, based on the catalytic performance of Sn–TiO_2 catalyst above, a possible mechanism was proposed and shown in Scheme 1. First, the free carbonyl radical generated from benzaldehyde, which would be attached with molecular oxygen to created perbenzoic acid intermediate. Subsequently, the peroxide intermediate reacted with the activated cyclohexanone by the Lewis acidic site on the Sn–TiO_2 catalyst [17, 18] to form the 'Criegee' type intermediate [5], followed by rearrangement to ε-caprolactone along with benzoic acid as by-product.

Conclusions

Ordered mesoporous xSn–TiO_2 catalysts with high tin species loading are designed and prepared by a one-pot EISA method and applied in the B–V oxidation of cyclohexanone by molecular oxygen in this paper. Tin species can be homogeneously tetrahedrally incorporated into the structure of ordered mesoporous TiO_2 supports and it can increase the Lewis acid amount. The 15Sn–TiO_2 catalyst shows highest catalytic performances, whose cyclohexanone conversion and ε-caprolactone selectivity is 91.4 and 93.2 %, respectively, and it has good reusable ability because the catalytic performance decreases slightly even after repeated reaction for 5 times. The possible mechanism was also proposed. This method provides a valuable reference of a promising catalyst for the B–V oxidation of cyclohexanone by molecular oxygen.

Acknowledgments This work was supported by Jiangsu Planned Projects for Post-doctoral Research Funds (1302121C); Open Project of Beijing Key Laboratory for Enze Biomass and Fine Chemicals; Project Funded by the Priority Academic Program Development of Jiangsu Higher Education Institutions.

References

1. Rahman S, Enjamuri N, Gomes R, Bhaumik A, Sen D, Pandey JK, Enjamuri S, Chowdhury B (2015) Appl Catal A 505:515–523
2. Alegria EC, Martins LM, Kirillova MV, Pombeiro AJ (2012) Appl Catal A 443:27–32
3. Jiménez-Sanchidrián C, Ruiz JR (2008) Tetrahedron Lett 64:2011–2026
4. Zhang G, Ren X, Zhang H, Peng Y, Gui S (2015) Catal Commun 58:59–63
5. Renz M, Meunier B (1999) Eur J Org Chem 4:737–750
6. Dutta B, Jana S, Bhunia S, Honda H, Koner S (2010) Appl Catal A 382:90–98
7. Jeong EY, Ansari MB, Park SE (2011) Acs Catal 1:855–863
8. Zang J, Ding Y, Yan L, Wang T, Lu Y, Gong L (2014) Catal Commun 51:24–28
9. Ma Y, Liang Z, Feng S, Zhang Y (2015) Appl Organomet Chem 29:450–455
10. Paul M, Pal N, Mondal J, Sasidharan M, Bhaumik A (2012) Chem Eng Sci 71:564–572
11. Geng L, Zhang X, Zhang W, Jia M, Liu G (2014) Chem Commun 50:2965–2967
12. Liu J, Qiao S, Hu Q (2011) Small 7:425–443
13. Teng W, Wu Z, Fan J, Chen H, Feng D, Lv Y, Wang J, Asiri AM, Zhao D (2013) Energy Environ Sci 6:2765–2776
14. Jeenpadiphat S, Björk EM, Odén M, Tungasmita DN (2015) J Mol Catal A 410:253–259
15. Corma A, Nemeth LT, Renz M, Valencia S (2001) Nature 412:423–425
16. Jiménez-Sanchidrián C, Hidalgo JM, Llamas R, Ruiz JR (2006) Appl Catal A 312:86–94
17. Corma A, Navarro MT, Renz M (2003) J Catal 219:242–246
18. Sasidharan M, Kiyozumi Y, Mal NK, Paul M, Rajamohanan PR, Bhaumik A (2009) Micropor Mesopor Mater 126:234–244
19. Taralkar US, Kalita P, Kumar R, Joshi PN (2009) Appl Catal A 358:88–94
20. Min H, Ran X, Fan J, Su Y, Yang J, Teng W, Zhang W, Li G, Zhao D (2015) J Mater Chem A 3:7399–7405
21. Zhou Z, Yu P, Qin J, Wu W, Xu L, Gu Z, Liu X (2016) J Porous Mater 23:239–245
22. Yang Y, Tian C (2015) Res Chem Intermed 41:5271–5281
23. Wang T, Yang G, Liu J, Yang B, Ding S, Yan Z, Xiao T (2014) Appl Surf Sci 311:314–323
24. Hamdy MS (2014) J Mol Catal A 393:39–46
25. Wang Y, Li B, Zhang C, Cui L, Kang S, Li X, Zhou L (2013) Appl Catal B 130:277–284
26. Xia C, Ju L, Zhao Y, Xu H, Zhu B, Gao F, Lin M, Dai Z, Zou X, Shu X (2015) Chin J Catal 36:845–854
27. Grosso D, Cagnol F, Soler-Illia G, Crepaldi EL, Amenitsch H, Bruneau AB, Bourgeois A, Sanchez C (2004) Adv Funct Mater 14:309–322

28. Li W, Zhao D (2013) Chem Commun 49:943–946
29. Pan D, Guo M, He M, Chen S, Wang X, Yu F, Li R (2014) J Mater Res 29:811–819
30. Zhang X, Zhang F, Chan K (2005) Appl Catal A 284:193–198
31. Miao Z, Zhao H, Yang J, Zhao J, Song H, Chou L (2014) Micropor Mesopor Mater 198:271–280
32. Li W, Bai Y, Liu C, Yang Z, Feng X, Lu X, Laak NK, Chan KY (2009) Environ Sci Technol 43:5423–5428
33. Yu M, Li C, Zeng G, Zhou Y, Zhang X, Xie Y (2015) Appl Surf Sci 342:174–182
34. Morris SM, Fulvio PF, Jaroniec M (2008) J Am Chem Soc 130:15210–15216
35. Chen M, Yang J, Liu Y, Li W, Fan J, Ran X, Teng W, Sun Y, Zhang W, Li G, Dou S, Zhao D (2015) J Mater Chem A 3:1405–1409
36. Kumar N, Hazarika SN, Limbu S, Boruah R, Deb P, Namsa ND, Das SK (2015) Micropor Mesopor Mater 213:181–187
37. Chen G, Ji S, Sang Y, Chang S, Wang Y, Hao P, Claverie J, Liu H, Yu G (2015) Nanoscale 7:3117–3125
38. Pachamuthu MP, Shanthi K, Luque R, Ramanathan A (2013) Green Chem 15:2158–2166
39. Zhang Q, Yang H, Yan W (2014) RSC Adv 4:56938–56944
40. Nabae Y, Rokubuichi H, Mikuni M, Kuang Y, Hayakawa T, Kakimoto M (2013) ACS Catal 3:230–236
41. Kaneda K, Ueno S, Imanaka T (1994) J Chem Soc, Chem Commun 25:797–798
42. Murahashi SI, Oda Y, Naota T (1992) Tetrahedron Lett 33:7557–7560
43. Ueno S, Ebitani K, Ookubo A, Kaneda K (1997) Appl Surf Sci 121:366–371
44. Llamas R, Jiménez-Sanchidrián C, Ruiz JR (2007) React Kinet Catal Lett 90:309–313